Iron deficiency modifies gene expression variation induced by augmented hypoxia sensing

Xu Zhang[1], **Wei Zhang**[2,3], **Shwu-Fan Ma**[4], **Galina Miasniakova**[5], **Adelina Sergueeva**[6], **Tatiana Ammosova**[7], **Min Xu**[7], **Sergei Nekhai**[7], **Mehdi Nourai**[7], **Michael S. Wade**[8,9], **Josef T. Prchal**[10], **Joe G. N. Garcia**[#8,9], **Roberto F. Machado**[#8,9], and **Victor R. Gordeuk**[#1]

[1]Comprehensive Sickle Cell Center, Section of Hematology/Oncology, Department of Medicine, University of Illinois at Chicago, Chicago, IL, USA

[2]Department of Pediatrics, University of Illinois at Chicago, Chicago, IL, USA

[3]Institute of Human Genetics, University of Illinois at Chicago, Chicago, IL, USA

[4]Section of Pulmonary/Critical Care, Department of Medicine, University of Chicago, Chicago, IL, USA

[5]Chuvash Republic Clinical Hospital 2, Cheboksary, Russian Federation, Howard University, Washington, DC

[6]Cheboksary Children's Hospital, Cheboksary, Russian Federation, Howard University, Washington, DC

[7]Center for Sickle Cell Disease, Howard University, Washington, DC

[8]Section of Pulmonary, Critical Care & Sleep Medicine, Department of Medicine, University of Illinois at Chicago, Chicago, IL, USA

[9]Institute for Personalized Respiratory Medicine, University of Illinois at Chicago, Chicago, IL, USA

[10]Departments of Medicine, Pathology and Genetics, University of Utah and VAH

Correspondence: Victor R. Gordeuk, MD, Suite 172, Clinical Sciences Building, 820 South Wood St., Chicago, IL 60612-7236 Tel 312-996-5680, Fax 312-996-5984, vgordeuk@uic.edu.

# These authors contributed equally to this work.

Abstract

In congenital Chuvash polycythemia (CP), VHL^{R200W} homozygosity leads to elevated hypoxia inducible factor (HIF) levels at normoxia. CP is often treated by phlebotomy resulting in iron deficiency, permitting us to examine the separate and synergistic effects of iron deficiency and HIF signaling on gene expression. We compared peripheral blood mononuclear cell gene expression profiles of eight VHL^{R200W} homozygotes with 17 wildtype individuals with normal iron status and found 812 up-regulated and 2120 down-regulated genes at false discovery rate 0.05. Among differential genes we identified three major gene regulation modules involving induction of innate immune responses, alteration of carbohydrate and lipid metabolism, and down-regulation of cell proliferation, stress-induced apoptosis and T-cell activation. These observations suggest molecular mechanisms for previous observations in CP of lower blood sugar without increased insulin and low oncogenic potential. Studies including 16 additional VHL^{R200W} homozygotes with low ferritin indicated that iron deficiency enhanced the induction effect of VHL^{R200W} for 50 genes including hemoglobin synthesis loci but suppressed the effect for 107 genes enriched for HIF-2 targets. This pattern is consistent with potentiation of HIF-1α protein stability by iron deficiency but a trend for down-regulation of HIF-2α translation by iron deficiency overriding an increase in HIF-2α protein stability.

Introduction

Hypoxia [1] and iron [2] modulate many metabolic processes. Chronic and acute hypoxia cause morbidity and mortality associated with pulmonary and brain edema [3], pulmonary hypertension [4] and aberrant metabolism [5; 6; 7]. Hypoxia has multiple effects on the expression of a vast array of genes, but this has been almost entirely investigated *in vitro* [8] or in experimental animals [9]. Iron deficiency is a common nutritional disorder, and it enhances pathways that are associated with hypoxia as iron is required for optimal activity of prolyl hydroxylases (PHDs) that are principal negative regulators of hypoxia inducible factors (HIFs) [10; 11]; iron deficiency also has hypoxia-unrelated metabolism-regulating roles [12; 13; 14; 15; 16]. Investigating the relationship between gene expression and the nutritional environment is important for understanding the complications of genetic disorders and for the development of optimal personalized approaches to medical care [17].

To better understand the pathological processes associated with hypoxia and to develop targeted intervention for disease states associated with hypoxia, we elected to define the hypoxia- and iron-related regulation of genes in humans *in vivo* by taking advantage of a congenital disorder of up-regulation of the hypoxic response at normoxia. Chuvash polycythemia (CP) is an autosomal recessive form of polycythemia/erythrocytosis that is endemic to the mid-Volga River region in the Russian Federation [18] and is characterized by increased levels of HIFs during normoxia [19]. Furthermore, CP is often accompanied by iron deficiency due to therapeutic phlebotomies, allowing us to weigh the effect of this common nutritional and environmental variable on hypoxic gene expression.

HIF-1 and HIF-2 are transcription factors that serve as master regulators of the hypoxic response. With normal oxygen tension, von Hippel Lindau (VHL) protein binds to HIF-α subunits and labels them for degradation by proteasomes. Proline hydroxylation of HIF-α by PHD enzymes is required for the interaction of HIF-α with VHL protein [20; 21]. Both oxygen and iron are needed for the activity of PHDs. Low oxygen inhibits VHL binding to HIF-α and activates HIF-dependent transcriptional responses, including increased erythropoiesis, angiogenesis, and a metabolic shift from oxidative phosphorylation to glycolysis for ATP generation. HIF-1α and HIF-2α may have complimentary but in some contexts also opposite effects on distinct gene targets depending on tissue- and cell-types [22; 23]. Iron deficiency also has the potential to exacerbate the hypoxic response due to its effect of impairing the activity of PHDs. Consistent with this possibility, iron chelating drugs post-translationally increase the α subunits of HIFs in cultured cells [10; 11], likely via PHD inhibition and apparently overriding a possible confounding effect of lack of iron in decreasing HIF-2α translation by promoting iron response proteins [24].

CP is characterized by a homozygous 598C>T (Arg200Trp or R200W) germline missense mutation in the *VHL* gene [19; 22], which leads to impaired activity of VHL protein to initiate ubiquitination and ultimately degradation of HIF-1α and HIF-2α. Patients with CP have increased levels of HIF-1 and HIF 2 during normoxia; this leads to altered expression of a large array of HIF-target genes, still not fully defined, and clinical manifestations that have so far been shown to include elevated hematocrit, lower systolic blood pressure (SBP) and enhanced risk of hemorrhage, thrombosis, pulmonary hypertension and other complications [25; 26]. In CP subjects iron deficiency would be predicted to further increase HIF-1α and HIF-2α and augment the increased HIF activity that occurs due to the genetic loss of VHL function [19; 20]; however, the opposite effect on HIF-2α mediated by its 5' iron responsive element [24] is also possible. The study of CP subjects might further clarify the role of iron deficiency in manifestations of the hypoxic response.

In this study we compared gene expression variation in peripheral blood mononuclear cells (PBMCs) between 24 *VHL^{R200W}* homozygotes and 21 Chuvash *VHL* wildtype controls. Those *VHL^{R200W}* homozygotes on a therapeutic phlebotomy are almost universally iron deficient. We therefore selected 17 healthy Chuvash *VHL* wildtype (WT) and 8 *VHL^{R200W}* homozygotes matched for serum ferritin concentration, and identified 2932 differentially expressed genes and related biological pathways attributable to the *VHL^{R200W}* mutation. We found that iron deficiency affected *VHL^{R200W}* induced gene expression possibly by distinct mechanisms.

Materials and Methods

Study Subjects

The Howard University IRB committee approved the protocol and each participant gave written informed consent. Twenty-one healthy Chuvash *VHL* wildtype (WT) control individuals and 24 Chuvash *VHL*^{R200W} homozygotes were recruited. The complete blood count was determined by an automated analyzer (Sysmex XT 2000i, Sysmex Corporation, Kobe, Hyogo, Japan), serum ferritin, serum erythropoietin (EPO), and plasma vascular

endothelial growth factor (VEGF) concentrations by enzyme linked immunosorbent assay (ELISA) (Ramco Laboratories Inc., Stafford, TX and R& D Systems, Minneapolis, MN).

RNA Isolation and Expression Profiling

Peripheral blood mononuclear cells (PBMCs) were isolated from EDTA whole blood Ficoll-Hypaque (GE, Pittsburgh, PA) density gradient centrifugation, washed with PBS, re-suspended in *Ambion RNAlater* (Invitrogen, Carlsbad, CA) solution, frozen at −80°C and shipped in liquid nitrogen from Cheboksary (Chuvashia, Russia) to Howard University. RNA was isolated using Trizol reagent (Invitrogen, CA) and the quality was assessed using nanodrop (Thermoscientific, Waltham, MA) and Agilent 2100 Bioanalyzer (Agilent Technologies, Palo Alto, CA). Total RNA was submitted to the University of Chicago Functional Genomics Center for whole transcript sense target labeling assay (Affymetrix, Inc., Santa Clara, CA), hybridization to the *Affymetrix GeneChip™* Human Exon 1.0 ST Array, and washing and scanning according to the manufacturer's procedure (Affymetrix, Inc., Santa Clara, CA).

Microarray data preprocessing

All 25mer probe sequences were aligned to human genome assembly GRCh37 allowing 2 mismatches [27]. Probes with perfect unique match to the genome were selected. We further removed probes that interrogate multiple gene transcripts and that contain SNPs with 1% minor allele frequency in dbSNP dataset (v135) [28]. Probe level intensities were $\log_2$ transformed, background corrected [29] and quantile normalized [30]. Probe intensity was subtracted by the corresponding probe mean across samples. Gene-level expression intensities were summarized as mean probe intensity within each transcript cluster. In total, 16,642 autosomal transcript clusters (gene-level) were included in this study.

Statistical analysis of clinical data and gene expression variation

Clinical variables were compared between *VHL* WT individuals and *VHL^{R200W}* homozygotes with Wilcoxon's rank sum test or Fisher's exact test. For comparison of gene expression, a linear model, gene expression level ~ genotype + error, was tested for each gene. A *d*-statistic [31] was calculated for the genotype effect. One hundred permutations were performed to estimate the false discovery rate (FDR) associated with the genotype effect [32]. Plasma concentrations of ferritin, EPO and VEGF were log transformed for correlation with gene expression level.

Identification of HIF-2 target genes

Public domain gene expression data for *VHL−/−* and *HIF1A−/−* renal clear cell carcinoma cell lines with and without HIF2A knocked down (4 *HIF2A* siRNA treated A498 cell samples verse 4 control siRNA treated A498 cell samples) [33] were compared. A similar probe signal preprocessing procedure and gene expression comparison approach described above was applied for the expression data using *Affymetrix GeneChip™* Human Gene 1.0 ST Array. A total of 525 HIF-2 target genes were detected at FDR of 0.10 which had lower expressed levels in *HIF2A* siRNA treated A498 cells than in control siRNA treated A498 cells.

Reactome gene interaction

Genes differentially regulated in VHL^{R200W} homozygotes were mapped to Reactome functional interaction database (2012 version) without linker genes. Gene network was constructed and clustered into sub-networks (modules). For each module, genes were ranked by the number of differential genes they interacted with within the module, and hub genes were defined as the top 20% genes.

Results

Clinical features of the study population

The clinical features of the study subjects (24 VHL^{R200W} homozygotes and 21 VHL WT) are summarized in Table 1A. Both age and gender were matched across the two groups. As expected red blood cell count (RBC), hemoglobin concentration (HGB) and hematocrit (HCT) were increased in VHL^{R200W} homozygotes. Nevertheless, the serum ferritin concentration was substantially reduced in 16 VHL^{R200W} patients (P <0.001), reflecting the fact that they had been treated with phlebotomy. Two HIF-regulated biomarkers, EPO and vascular endothelial growth factor (VEGF), were increased in VHL^{R200W} homozygotes (P <0.001 and P = 0.039, respectively), consistent with previous reports [26].

PBMC transcriptional responses to constitutively activated HIF in VHL^{R200W} homozygotes

A total of 16,642 genes were analyzed for 24 VHL^{R200W} homozygotes and 21 VHL WT individuals at normoxia. At a genome-wide false discover rate (FDR) of 0.05, almost 10,000 genes exhibited altered regulation in the VHL^{R200W} homozygotes, predominantly a modest up-regulation (Figure 1A). As many VHL^{R200W} homozygotes regularly undergo phlebotomy, serum ferritin concentrations were substantially lower in VHL^{R200W} homozygotes than in WT individuals (Table 1A). Thus the detected expression difference could be attributed to genotype and/or iron variation. To assess the relative contribution of these two effects, we analyzed the expression data for the top 3366 differential genes (0.01 FDR) by a linear model including both genotype and serum ferritin concentration as explanatory variables. With ferritin variation being accounted for, genotype effect was no longer significant for 1336 genes at nominal P=0.05 (Figure 1B), suggesting that iron status, reflected as serum ferritin concentration, confounds genotype effect for a substantial proportion of genes. We thus selected for final analysis 17 control subjects and 8 VHL^{R200W} homozygotes (Table 1B) who were iron sufficient (serum ferritin concentration   21 μg/L) and matched for age (P=0.9) and gender (P >0.9). At a genome-wide FDR of 0.05, 2932 differential genes were detected (Figure 1C), with 812 genes up regulated (Supplemental Table 1) and 2120 genes down regulated (Supplemental Table 2) in VHL^{R200W} homozygotes. Genes differentially regulated in VHL^{R200W} homozygotes by   1.5 fold are listed in Table 2. As a validation of microarray measurements, we regressed plasma VEGF concentrations on expression levels of $VEGFA$ among 24 VHL^{R200W} homozygotes. We found significant correlations between the two measurements (r^2=0.18, P=0.04).

The VHL^{R200W} mutation causes constitutive stabilization of both HIF-1 and HIF-2, which play overlapping roles in hypoxia transcription responses, each with certain target preferences [34]. Genes up-regulated in PBMCs of VHL^{R200W} homozygotes were enriched

in HIF-1 target genes that were experimentally validated in previous publications (Table S2 in [34]) by 4.8-fold (binomial test $P=2\times10^{-8}$), and in HIF-1 target genes revealed by expression profiling of arterial endothelial cells [8] by 2.0 fold (P=0.007). Genes induced in VHL^{R200W} homozygotes were also enriched in HIF-2 preferred target genes in an expression profiling of human umbilical vein endothelial cells [35] by 2.5-fold (P=0.0001). We further identified 525 genes as HIF-2 targets (FDR 0.10) from the published expression dataset in which $HIF2A$ was knocked down in $VHL–/–$ and $HIF1A–/–$ renal clear cell carcinoma cell lines [33]; genes induced by VHL^{R200W} were enriched in these HIF-2 targets by 1.9-fold (P=2×10^{-5}).

Genes up-regulated in PBMCs of VHL^{R200W} homozygotes were enriched in Gene Ontology (GO) biological processes of inflammatory response, response to lipopolysaccharide, response to bacteria, response to virus, regulation of cytokine production, chemotaxis, regulation of anatomical structure morphogenesis, regulation of cellular catabolic process, positive regulation of cell communication, wound healing, endocytosis, regulation of myeloid cell differentiation, regulation of smooth muscle cell proliferation, and positive regulation of anti-apoptosis (Figure 2). IL6, IL1B, TNF, TLR4, HMOX1, NOD2, IL10, SLC11A1, THBS1 and *EREG* are involved in many of these biological processes. Genes down-regulated in VHL^{R200W} homozygotes were enriched in GO biological processes of RNA metabolic process, RNA processing, RNA transport, translation, chromatin organization, and methylation (Figure 2).

Gene regulation networks in VHL^{R200W} homozygotes

To reveal the gene regulation cascades triggered by homozygous VHL^{R200W} mutation, we mapped the 2932 differentially expressed genes to the REACTOME functional interaction database [36] and identified three major regulatory modules (Supplemental Table 3). We ranked genes by the number of differential genes with which they interacted within the module and defined hub genes as the top 20% genes for each module. Module 1 covers 266 differential genes (Figure 3A). The up-regulated hub genes *RXRA, CEBPA, RARA* and *PRIC285* are involved in transcriptional activation of genes involved in lipid metabolism in liver and adipose tissue [37]. The down-regulation of hub genes *SMAD4* and *SMAD2* and up-regulation of *SMAD7* indicated a suppression of TGF-β signaling, which in turn was related to up-regulation of several cell proliferation suppressors, *CDKN1A, E2F4* and *PML*, as well as up-regulation of *TCF7L2* whose genetic variants associate with risk of type 2 diabetes mellitus [38]. Among the hub genes of this module, there was an over-representation of genes that function through epigenetic mechanisms, for instance *HDAC2, HDAC1, CTCF, NCOR1* and *CARM1*.

Module 2 covers 223 differential genes (Figure 3B). T cell receptor signaling pathways were suppressed as indicated by down-regulation of genes encoding the TCR/CD3 complex subunits *CD3D, CD3E, CD3G* and *CD247*, as well as *CD28* that encodes a T cell co-stimulator. These observations are consistent with our previous observations of lower peripheral blood concentrations of CD4 positive T-helper cells and lower CD4/CD8 ratio in VHL^{R200W} homozygotes [39]. The down-regulation of *PIK3CA* and *PIK3R1* may also associate with the suppression of T-cell proliferation. The up-regulation of *FCGR2A, HCK,*

GAB2 and *ITGB2* suggested up-regulation of phagocytosis, the up-regulation of *RHOG*, *RRAS* and *FES* enhanced cytoskeleton remodeling and cell-cell adhesion, and the up-regulation of *STAT2* transcriptional activation of interferon-stimulated genes in this module.

Module 3 covers 187 differential genes (Figure 3C). Genes encoding pro-inflammatory cytokines *TNF* and *IL1B* were up-regulated, as was *TLR4*, an innate immune regulator. Cell survival was up-regulated, as suggested by up-regulation of *AKT1* that mediates survival signaling and *BCL2L1* that inhibits cell death by regulating outer mitochondrial membrane channel opening. Consistently, Fas-mediated apoptosis was suppressed as suggested by the down-regulation of *CASP8* and *CASP2* and the down-regulation of *MAP3K7* and *MAPK8* that mediate stress-induced apoptosis. There were several additional gene modules with smaller size identified in genes differentially expressed in *VHL^R200W* homozygotes (Supplemental Table 3). Overall these smaller modules suggested suppression of transcription, translation, DNA replication, DNA repair and mitosis in *VHL^R200W* homozygotes.

Iron deficiency modifies the PBMC transcriptional responses to constitutively activated HIF in VHL^R200W homozygotes

To assess the influence of iron deficiency due to phlebotomy on homozygous *VHL^R200W*-triggered transcriptional responses, we evaluated the effect of serum ferritin concentration variation on those 2931 differential genes detected at FDR 0.05 in 24 *VHL^R200W* homozygotes (8 iron sufficient subjects plus an additional 16 iron deficient subjects). Expression of genes up-regulated in *VHL^R200W* homozygotes was influenced by serum ferritin concentration compared to genes down-regulated or genes with no significant difference (Figure 4A). Specifically, among the 812 up-regulated genes low serum ferritin enhanced the induction effect for 50 genes in *VHL^R200W* homozygotes (Spearman's rank test *P* <0.05, Table 3). These genes included *BCL2L1, BNIP3L, FKBP8* and *SNCA* that involved in gene module 3 for regulation of mitochondria-mediated apoptosis. The low iron enhanced genes also included hemoglobin (*HBB, HBD, HBM, HBQ1)* and heme synthesis (*FECH, SLC25A37, SLC25A39*) loci, alpha hemoglobin stabilizing protein (*AHSP*), genes encoding erythrocyte cytoskeleton and membrane components (*SPTB, ANK1, SLC4A1, EPB49, EPB42* and *TMOD1*), genes involved in carbon dioxide transport in erythrocytes *(CA1, SLC4A1)*, and the hemoglobin oxygen affinity regulator, biphosphate glycerate mutase (*BPGM*). Previous studies had reported HBB expression in non-erythroid cells including up-regulation by hypoxia [40; 41]. In addition to an inverse correlation with serum ferritin concentration, the expression of these genes positively correlated with serum erythropoietin (EPO) concentration (Supplemental Figure 1).

Unexpectedly, low serum ferritin concentration was associated with lower expression of 107 genes up-regulated in *VHL^R200W* homozygotes (Table 4). Compared to the strong induction effect of iron deficiency (Supplemental Figure 2), the magnitude of the suppressive effect of iron deficiency on *VHL^R200W* up-regulated genes was generally mild (Supplemental Figure 3). Among these genes were several hub genes of the major gene regulation modules, including *RARA, VDR, PML* and *TCF7L2* in module 1, *ITGB2, RHOG* and *STAT2* in module 2, and *AKT1* in module 3. In addition, many *VHL^R200W* up-regulated genes that were

suppressed by low iron were involved in the innate immune response and lysozyme activity (see Table 4)).

Although iron deficiency is expected to enhance HIF-1α and HIF-2α levels and related transcriptional activity by decreasing prolyl hydroxylase activity [1], it could reduce HIF-2-mediated transcription through IRP-mediated suppression of HIF-2α translation [42]. Consistent with this possible IRP-mediated decrease in HIF-2α mechanism, 100 HIF-2 target genes [33] that exhibited >1.08 fold change in VHL^{R200W} homozygotes had significantly more positive correlations with serum ferritin concentrations than 2282 non-HIF-2 target genes with the same fold induction in VHL^{R200W} homozygotes (one-sided Kolmogorov-Smirnov test P=0.0002, Figure 4B). Examples of hypoxia-induced genes that were enhanced or suppressed by iron deficiency are presented in Figure 5.

Discussion

Investigating the relationship between gene expression and environmental factors such as nutritional variables is important for understanding the selection advantages and disadvantages of genetic disorders and for developing personalized approaches to medical care [17]. Chronic hypoxia and acute hypoxia are associated with pulmonary and brain edema [3], pulmonary hypertension [4], aberrant metabolism [5; 6; 7], and increased mortality. Hypoxia has diverse effects on gene expression as investigated in cells in vitro [8], and lack of iron can further enhance pathways that are associated with hypoxia [10; 11]. To better understand the pathological processes associated with hypoxia we evaluated the expression of genes in individuals with CP, VHL^{R200W} homozygotes with increased levels of hypoxia inducible factors (HIFs) during normoxia [19]. Furthermore, VHL^{R200W} homozygotes often have iron deficiency due to therapeutic phlebotomies, allowing us to weigh the effect of this common nutritional and environmental variable on hypoxic gene expression. We found that the chronic hypoxic response in VHL^{R200W} homozygotes under normoxia induced profound expression alterations in PBMCs that affect inflammation, metabolism, cell survival and cell proliferation. Furthermore, iron deficiency augments expression of HIF-1α preferred target genes whereas represses expression of potential HIF-2α preferred targets in VHL^{R200W} homozygotes.

We recently reported that CP is characterized by lower blood glucose concentrations, likely related to decreased hepatic gluconeogenesis and increased skeletal muscle uptake and glycolysis [43]. The gene regulation module 1 revealed in this study provides further insights into the effect of VHL^{R200W} homozygosity on metabolic pathways. Macrophages derived from peripheral blood mononuclear cells have an important role in metabolic pathways in the liver, pancreas and adipose tissue [44], and several up-regulated genes (*RXRA, CEBPA, BACH1* and *MAFB*) are essential for macrophage-associated gene expression[45]. The up-regulation of *TCF7L2* may prevent glucose intolerance by suppression of gluconeogenesis in liver [46] and stimulation of glucose up-take by peripheral organs, which is supported by decreased liver expression of *Slc2a2* and *G6pc* but increased skeleton muscle expression of *Slc2a1* in CP mice [43]. The up-regulation of *RXRA, CEBPA, RARA* and *PRIC285* in VHL^{R200W} homozygotes suggests a stimulation of peroxisomal beta oxidation mediated by PPARA in liver [47]. Concurrently, the up-

regulation of *ADIPOR1*suggests increased fatty acid oxidation in adipose tissues. Generally increased lipid degradation in liver and adipose tissues may cause elevated serum glycerol and triglyceride concentrations previously observed in CP patients [43].

The lack of increased incidence of cancer in *VHL^R200W* homozygotes is striking because they have reduced activity of the *VHL* tumor suppressive gene in all cells since birth, along with increased levels of HIFs and VEGF that have been implicated in oncogenesis. The Warburg effect stipulates that cancer cells are highly dependent on glycolysis rather than oxidative phosphorylation for energy production [48], and hypoxia is also associated with a shift to anaerobic glycolysis [49]. Consistently, we found down-regulation of genes involved in aerobic energy production (e.g. *SDHD, NDUFA4, COX7A2, ATP5L*) and up-regulation of genes involved in glycolysis (e.g. *HK3, ALDOA, LDHA)* in PBMCs of CP subjects. However the unexpected down-regulation of three known hypoxia-induced genes, *PDK1, BNIP3* and *ETS1*, which in general suppress mitochondrial function and promote anaerobic glycolysis [50; 51; 52], may imply preservation of oxidative phosphorylation in CP and a potential mechanism for protection from cancer [49; 52; 53]. The up-regulation of several tumor suppressor genes (*CDKN1A, E2F4, PML*), as well as altered expression of markers associated with cancer outcome (S*ELENBP1* [54] and *L DHB* [55] may also help explain a cancer-protective effect of *VHL^R200W* homozygosity. Activation of T-cells involves rapid clonal expansion, which is to a certain extent similar to cancer cells in that it depends on glycolysis for both energy and biosynthetic substrates [56]. Therefore, the suppression of T-cell activation could also be related to a metabolic profile less hospitable to oncogenesis.

The up-regulation of inflammatory and innate immune responses in gene regulation module 3 is consistent with our previous report of increased plasma concentrations of Th1 and Th2 cytokines in CP [39]. This regulation module is also likely related to macrophage activation [44], as suggested by the up-regulation of hub gene *SPI1* and gene *ETS2* which are key regulators of macrophage differentiation [44]. Pro- and anti-inflammatory cytokines and innate immune response genes typically derived from macrophages, for instance *TNF, IL1B, IL6, IL10, TLR4* and *CD14*, were up-regulated in this module, as were several macrophage-associated markers *MSR1, CD68* and *CD163*. Therefore both pro-inflammatory (M1) macrophages and anti-inflammatory (M2) macrophages appeared to be activated in CP patients.

Mechanistically, low iron suppresses PHD activity and therefore enhances both HIF-1α and HIF-2α stability. On the other hand, a down regulation of HIF-2α translation could override the activation for HIF-2α preferred target genes [24], as illustrated in Figure 6. Therefore genes enhanced by low iron were potential HIF-1 targets while genes suppressed by low iron were potential HIF-2 targets, which is supported by expression correlations with serum ferritin concentration between empirically defined HIF-2 targets and non HIF-2 targets (Figure 4B). *VHL^R200W*-induced genes exhibited a greater tendency to be influenced by iron fluctuation compared with the suppressed genes (Figure 4A). This is consistent with the conclusion that genes down-regulated by hypoxia are typically not direct HIF target genes [57]. Notably, the *VHL^R200W*-induced genes were biased toward a positive correlation with iron status as reflected in serum ferritin concentration, while genes called as no difference (FDR   0.05) exhibited a mild negative correlation with iron status (Figure 4A), probably

because many of the latter were modestly up-regulated in CP. Overall, these observations suggest that in CP patients genes most strongly induced in PBMCs tend to be HIF-2 preferred targets.

Since the suppressive effects of low iron on HIF-2 targets appeared to result from an equilibrium between PHD related HIF-2 stabilization and IRP related decrease in HIF-2 translation, such effects observed in PBMCs are likely contributed primarily by cells sensitive to iron fluctuation, in particular, monocytes that are the precursors to tissue macrophages, the major iron storage cells of the body. Notably, many of the HIF-1 targets strongly enhanced by low iron status are involved in erythrocyte function. Phlebotomy-associated iron deficiency could influence various aspects of physiology in CP. For instance, iron deficiency suppressed expression of *TCF7L2* which potentially modulates the risk of diabetes and cardiovascular disease [58], but enhanced expression of *BCL2L1*, a gene inhibiting mitochondria-mediated cell death, suggesting promotion of cell survival [59]. Although optimal delineation of HIF-1 and HIF-2 gene regulation needs cell-specific expression studies, the securing of PBMCs was noninvasive, simple and practical and acceptable to the study subjects as this was virtually risk-free and there was only minimal discomfort.

In conclusion, our findings are consistent with a divergent effect of iron deficiency on expression of genes in PBMCs according to whether the gene is predominantly regulated by HIF-1 versus HIF-2 as depicted in Figure 6, but further research is needed to confirm the molecular basis of this observation. Further research to define the relative risks and benefits of therapeutic phlebotomy for polycythemia is also in order in the light of our gene expression observations. The elucidation of the genomic pathways affecting predisposition to thromboses, pulmonary hypertension, lower SBP and the interaction of augmented hypoxia sensing with iron deficiency in CP should have broad implications for understanding of the pathophysiology of many diseases and the development of targeted therapies of many human maladies.

Supplementary Material

Refer to Web version on PubMed Central for supplementary material.

Acknowledgements

References

1. Semenza GL. Hypoxia-inducible factors in physiology and medicine. Cell. 2012; 148:399–408. [PubMed: 22304911]

2. Bothwell, T.; Charlton, RW.; Cook, JD.; Finch, CA. Iron Metabolism in Man. Blackwell Scientific Publications; Oxford: 1979.

3. Richalet JP, Larmignat P, Poitrine E, Letournel M, Canoui-Poitrine F. Physiological risk factors for severe high-altitude illness: a prospective cohort study. Am J Respir Crit Care Med. 2012; 185:192–8. [PubMed: 22071330]

4. Smith TG, Balanos GM, Croft QP, et al. The increase in pulmonary arterial pressure caused by hypoxia depends on iron status. J Physiol. 2008; 586:5999–6005. [PubMed: 18955380]

5. Bailey DM, Bartsch P, Knauth M, Baumgartner RW. Emerging concepts in acute mountain sickness and high-altitude cerebral edema: from the molecular to the morphological. Cell Mol Life Sci. 2009; 66:3583–94. [PubMed: 19763397]

6. Martin DS, Ince C, Goedhart P, Levett DZ, Grocott MP. Abnormal blood flow in the sublingual microcirculation at high altitude. Eur J Appl Physiol. 2009; 106:473–8. [PubMed: 19333616]

7. Scrase E, Laverty A, Gavlak JC, et al. The Young Everest Study: effects of hypoxia at high altitude on cardiorespiratory function and general well-being in healthy children. Arch Dis Child. 2009; 94:621–6. [PubMed: 19395400]

8. Manalo DJ, Rowan A, Lavoie T, et al. Transcriptional regulation of vascular endothelial cell responses to hypoxia by HIF-1. Blood. 2005; 105:659–69. [PubMed: 15374877]

9. Yuan G, Khan SA, Luo W, et al. Hypoxia-inducible factor 1 mediates increased expression of NADPH oxidase-2 in response to intermittent hypoxia. J Cell Physiol. 2011; 226:2925–33. [PubMed: 21302291]

10. Chan DA, Sutphin PD, Denko NC, Giaccia AJ. Role of prolyl hydroxylation in oncogenically stabilized hypoxia-inducible factor-1alpha. J Biol Chem. 2002; 277:40112–7. [PubMed: 12186875]

11. Park SS, Bae I, Lee YJ. Flavonoids-induced accumulation of hypoxia-inducible factor (HIF)-1alpha/2alpha is mediated through chelation of iron. J Cell Biochem. 2008; 103:1989–98. [PubMed: 17973296]

12. Collins JF, Franck CA, Kowdley KV, Ghishan FK. Identification of differentially expressed genes in response to dietary iron deprivation in rat duodenum. Am J Physiol Gastrointest Liver Physiol. 2005; 288:G964–71. [PubMed: 15637178]

13. Fry MM, Kirk CA, Liggett JL, et al. Changes in hepatic gene expression in dogs with experimentally induced nutritional iron deficiency. Vet Clin Pathol. 2009; 38:13–9. [PubMed: 19228364]

14. Hu CJ, Wang LY, Chodosh LA, Keith B, Simon MC. Differential roles of hypoxia-inducible factor 1alpha (HIF-1alpha) and HIF-2alpha in hypoxic gene regulation. Mol Cell Biol. 2003; 23:9361–74. [PubMed: 14645546]

15. Karlovich C, Duchateau-Nguyen G, Johnson A, et al. A longitudinal study of gene expression in healthy individuals. BMC Med Genomics. 2009; 2:33. [PubMed: 19500411]

16. O'Rourke JA, Nelson RT, Grant D, et al. Integrating microarray analysis and the soybean genome to understand the soybeans iron deficiency response. BMC Genomics. 2009; 10:376. [PubMed: 19678937]

17. Kaput J, Rodriguez RL. Nutritional genomics: the next frontier in the postgenomic era. Physiol Genomics. 2004; 16:166–77. [PubMed: 14726599]

18. Polyakova L. Familial erythrocytosis among inhabitants of the Chuvash ASSR. Problemi Gematologii I perelivaniya Krovi. 1974; 10:30–6.

19. Ang SO, Chen H, Hirota K, et al. Disruption of oxygen homeostasis underlies congenital Chuvash polycythemia. Nat Genet. 2002; 32:614–21. [PubMed: 12415268]

20. Kaelin WG Jr. Ratcliffe PJ. Oxygen sensing by metazoans: the central role of the HIF hydroxylase pathway. Mol Cell. 2008; 30:393–402. [PubMed: 18498744]

21. Minamishima YA, Kaelin WG Jr. Reactivation of hepatic EPO synthesis in mice after PHD loss. Science. 2010; 329:407. [PubMed: 20651146]

22. Hickey MM, Lam JC, Bezman NA, Rathmell WK, Simon MC. von Hippel-Lindau mutation in mice recapitulates Chuvash polycythemia via hypoxia-inducible factor-2alpha signaling and splenic erythropoiesis. J Clin Invest. 2007; 117:3879–89. [PubMed: 17992257]

23. Rankin EB, Rha J, Unger TL, et al. Hypoxia-inducible factor-2 regulates vascular tumorigenesis in mice. Oncogene. 2008; 27:5354–8. [PubMed: 18490920]

24. Sanchez M, Galy B, Muckenthaler MU, Hentze MW. Iron-regulatory proteins limit hypoxia-inducible factor-2alpha expression in iron deficiency. Nat Struct Mol Biol. 2007; 14:420–6. [PubMed: 17417656]

25. Bushuev VI, Miasnikova GY, Sergueeva AI, et al. Endothelin-1, vascular endothelial growth factor and systolic pulmonary artery pressure in patients with Chuvash polycythemia. Haematologica. 2006; 91:744–9. [PubMed: 16769575]

26. Gordeuk VR, Sergueeva AI, Miasnikova GY, et al. Congenital disorder of oxygen sensing: association of the homozygous Chuvash polycythemia VHL mutation with thrombosis and vascular abnormalities but not tumors. Blood. 2004; 103:3924–32. [PubMed: 14726398]

27. Langmead B, Salzberg SL. Fast gapped-read alignment with Bowtie 2. Nat Methods. 2012; 9:357–9. [PubMed: 22388286]

28. Sherry ST, Ward MH, Kholodov M, et al. dbSNP: the NCBI database of genetic variation. Nucleic Acids Res. 2001; 29:308–11. [PubMed: 11125122]

29. Borevitz JO, Liang D, Plouffe D, et al. Large-scale identification of single-feature polymorphisms in complex genomes. Genome Res. 2003; 13:513–23. [PubMed: 12618383]

30. Irizarry RA, Hobbs B, Collin F, et al. Exploration, normalization, and summaries of high density oligonucleotide array probe level data. Biostatistics. 2003; 4:249–64. [PubMed: 12925520]

31. Tusher VG, Tibshirani R, Chu G. Significance analysis of microarrays applied to the ionizing radiation response. Proc Natl Acad Sci U S A. 2001; 98:5116–21. [PubMed: 11309499]

32. Anderson M. Permutation tests for univariate or multivariate analysis of variance and regression. Canadian Journal of Fisheries and Aquatic Sciences. 2001; 58:626–39.

33. Bertout JA, Majmundar AJ, Gordan JD, et al. HIF2alpha inhibition promotes p53 pathway activity, tumor cell death, and radiation responses. Proc Natl Acad Sci U S A. 2009; 106:14391–6. [PubMed: 19706526]

34. Benita Y, Kikuchi H, Smith AD, et al. An integrative genomics approach identifies Hypoxia Inducible Factor-1 (HIF-1)-target genes that form the core response to hypoxia. Nucleic Acids Res. 2009; 37:4587–602. [PubMed: 19491311]

35. Nagao K, Oka K. HIF-2 directly activates CD82 gene expression in endothelial cells. Biochem Biophys Res Commun. 2011; 407:260–5. [PubMed: 21382346]

36. Vastrik I, D'Eustachio P, Schmidt E, et al. Reactome: a knowledge base of biologic pathways and processes. Genome Biol. 2007; 8:R39. [PubMed: 17367534]

37. Keller H, Dreyer C, Medin J, et al. Fatty acids and retinoids control lipid metabolism through activation of peroxisome proliferator-activated receptor- retinoid X receptor heterodimers. Proc Natl Acad Sci U S A. 1993; 90:2160–4. [PubMed: 8384714]

38. Grant SF, Thorleifsson G, Reynisdottir I, et al. Variant of transcription factor 7-like 2 (TCF7L2) gene confers risk of type 2 diabetes. Nat Genet. 2006; 38:320–3. [PubMed: 16415884]

39. Niu X, Miasnikova GY, Sergueeva AI, et al. Altered cytokine profiles in patients with Chuvash polycythemia. Am J Hematol. 2009; 84:74–8. [PubMed: 19062180]

40. Liu L, Zeng M, Stamler JS. Hemoglobin induction in mouse macrophages. Proc Natl Acad Sci U S A. 1999; 96:6643–7. [PubMed: 10359765]

41. Grek CL, Newton DA, Spyropoulos DD, Baatz JE. Hypoxia up-regulates expression of hemoglobin in alveolar epithelial cells. Am J Respir Cell Mol Biol. 2011; 44:439–47. [PubMed: 20508070]

42. Zimmer M, Lamb J, Ebert BL, et al. The connectivity map links iron regulatory protein-1-mediated inhibition of hypoxia-inducible factor-2a translation to the anti- inflammatory 15-deoxy-delta12,14-prostaglandin J2. Cancer Res. 2010; 70:3071–9. [PubMed: 20354189]

43. McClain DA, Abuelgasim KA, Nouraie M, et al. Decreased serum glucose and glycosylated hemoglobin levels in patients with Chuvash polycythemia: a role for HIF in glucose metabolism. J Mol Med (Berl). 2013; 91:59–67. [PubMed: 23015148]

44. Wynn TA, Chawla A, Pollard JW. Macrophage biology in development, homeostasis and disease. Nature. 2013; 496:445–55. [PubMed: 23619691]

45. Gautier EL, Shay T, Miller J, et al. Gene-expression profiles and transcriptional regulatory pathways that underlie the identity and diversity of mouse tissue macrophages. Nat Immunol. 2012; 13:1118–28. [PubMed: 23023392]

46. Vaquero AR, Ferreira NE, Omae SV, et al. Using gene-network landscape to dissect genotype effects of TCF7L2 genetic variant on diabetes and cardiovascular risk. Physiol Genomics. 2012; 44:903–14. [PubMed: 22872755]

47. Pinaire JA, Reifel-Miller A. Therapeutic potential of retinoid x receptor modulators for the treatment of the metabolic syndrome. PPAR Res. 2007; 2007:94156. [PubMed: 17497022]

48. Warburg O. On the origin of cancer cells. Science. 1956; 123:309–14. [PubMed: 13298683]

49. Semenza GL. Regulation of cancer cell metabolism by hypoxia-inducible factor 1. Semin Cancer Biol. 2009; 19:12–6. [PubMed: 19114105]

50. Kim JW, Tchernyshyov I, Semenza GL, Dang CV. HIF-1-mediated expression of pyruvate dehydrogenase kinase: a metabolic switch required for cellular adaptation to hypoxia. Cell Metab. 2006; 3:177–85. [PubMed: 16517405]

51. Regula KM, Ens K, Kirshenbaum LA. Inducible expression of BNIP3 provokes mitochondrial defects and hypoxia-mediated cell death of ventricular myocytes. Circ Res. 2002; 91:226–31. [PubMed: 12169648]

52. Verschoor ML, Wilson LA, Verschoor CP, Singh G. Ets-1 regulates energy metabolism in cancer cells. PLoS One. 2010; 5:e13565. [PubMed: 21042593]

53. Hitosugi T, Fan J, Chung TW, et al. Tyrosine phosphorylation of mitochondrial pyruvate dehydrogenase kinase 1 is important for cancer metabolism. Mol Cell. 2011; 44:864–77. [PubMed: 22195962]

54. Chen G, Wang H, Miller CT, et al. Reduced selenium-binding protein 1 expression is associated with poor outcome in lung adenocarcinomas. J Pathol. 2004; 202:321–9. [PubMed: 14991897]

55. Zha X, Wang F, Wang Y, et al. Lactate dehydrogenase B is critical for hyperactive mTOR-mediated tumorigenesis. Cancer Res. 2011; 71:13–8. [PubMed: 21199794]

56. Wang R, Green DR. Metabolic checkpoints in activated T cells. Nat Immunol. 2012; 13:907–15. [PubMed: 22990888]

57. Mole DR, Blancher C, Copley RR, et al. Genome-wide association of hypoxia inducible factor (HIF)-1alpha and HIF-2alpha DNA binding with expression profiling of hypoxia-inducible transcripts. J Biol Chem. 2009; 284:16767–75. [PubMed: 19386601]

58. Grundy SM, Barlow CE, Farrell SW, Vega GL, Haskell WL. Cardiorespiratory fitness and metabolic risk. Am J Cardiol. 2012; 109:988–93. [PubMed: 22221951]

59. Lenihan CR, Taylor CT. The impact of hypoxia on cell death pathways. Biochem Soc Trans. 2013; 41:657–63. [PubMed: 23514172]

60. Benjamini Y, Hochberg Y. Controlling the false discovery rate: a practical and powerful approach to multiple testing. Journal of the Royal Statistical Society Series B. 1995:289–300.
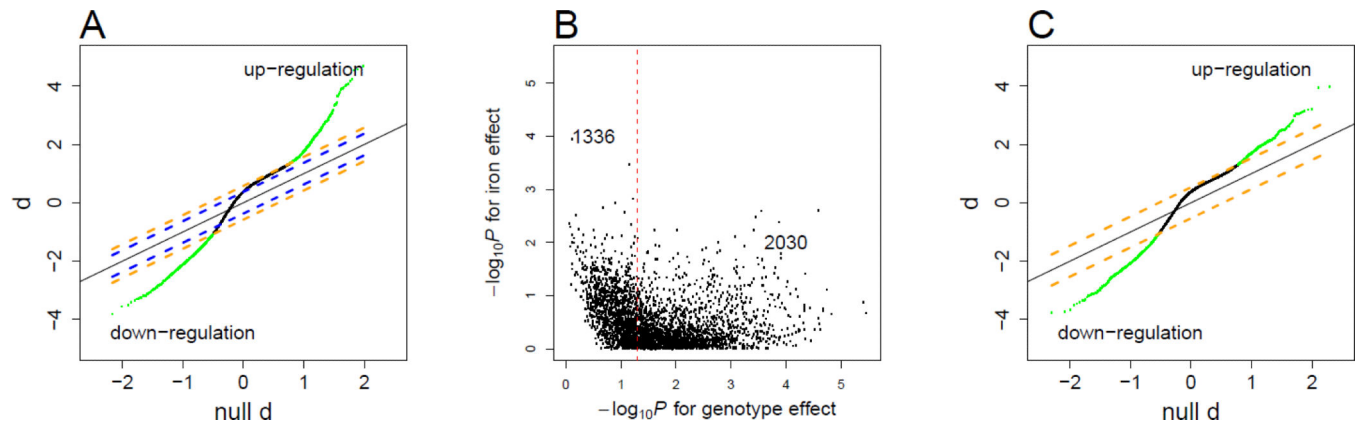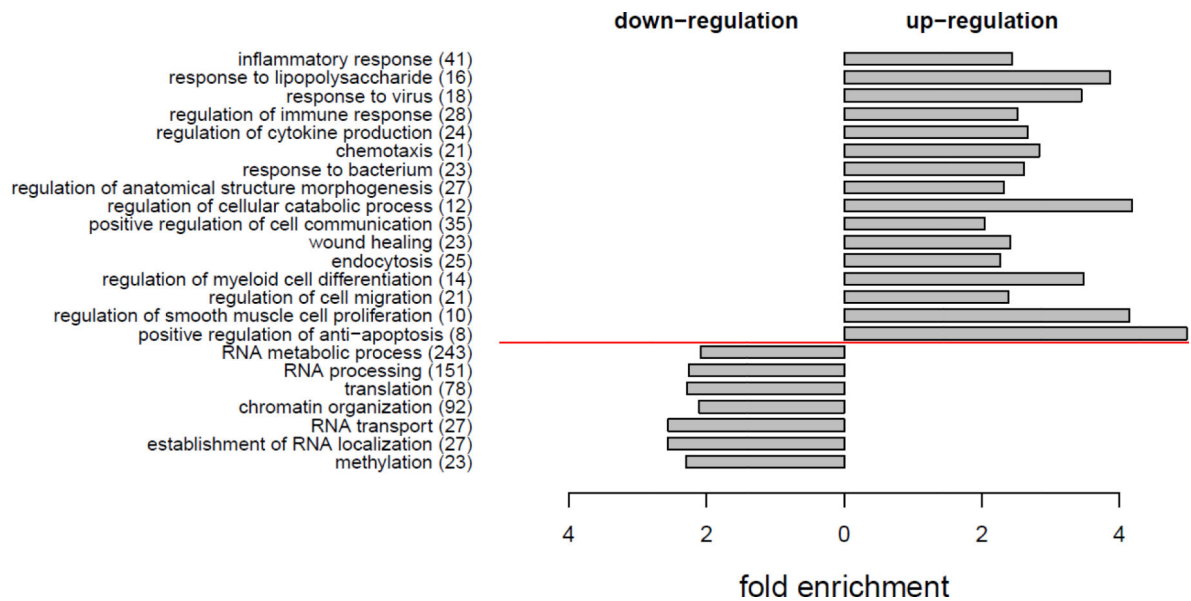
Figure 1.
Detection of genes differentially expressed between VHL^{R200W} homozygotes and VHL wildtype control individuals.

A. The quantile-quantile plot for d-statistic of differential expression between 21 WT individuals and 24 VHL^{R200W} homozygotes without controlling for serum ferritin variation. Blue lines represent d-statistic cutoffs for calling genes at FDR 0.05 and orange lines at FDR 0.01. Solid black line represents diagonal. Green points represent significant calls at FDR 0.01. The majority of genes exhibit a modest up-shift relative to the diagonal line at FDR 0.05, implying up-regulation.

B. For genes called at FDR 0.01 in A, expression level was fitted by a linear model including VHL genotype and log (ferritin) as two explanatory variables; for 1336 genes, genotype effect was no longer significant at nominal $P = 0.05$. This indicates that ferritin variation confounded genotype effect.

C. The quantile-quantile plot for d-statistic of differential expression between 17 WT individuals and 8 VHL^{R200W} homozygotes matched for serum ferritin concentration. Orange lines represent d-statistic cutoffs for calling genes at FDR 0.05. Green points represent significant calls at FDR 0.05.
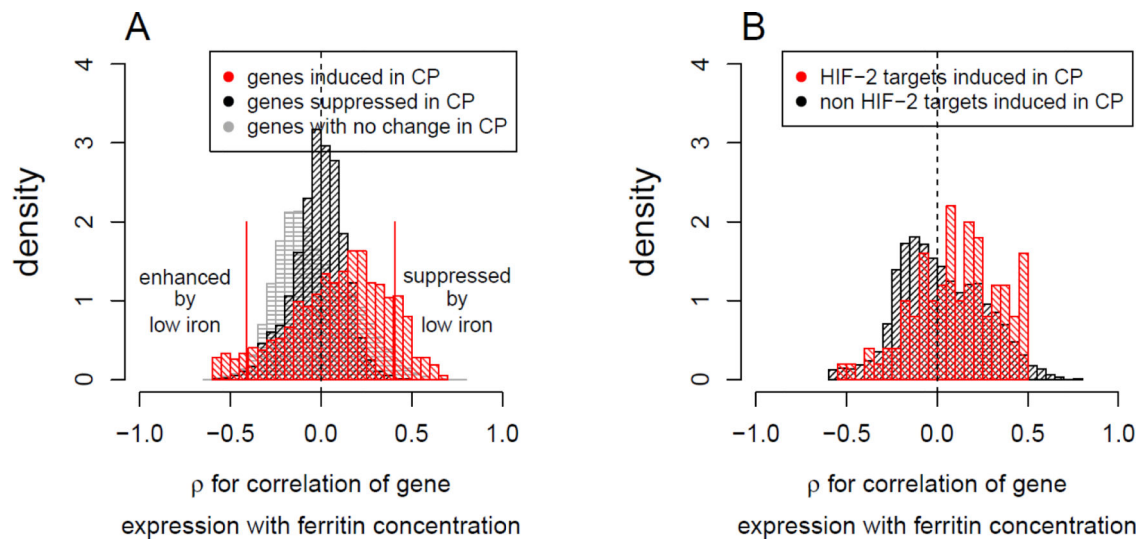
Figure 2.
Gene Ontology (GO) analysis for the 2932 differential genes detected between 17 *VHL* WT and 8 *VHL^R200W* homozygote individuals matched for serum ferritin concentration. Genes up-regulated (812) or down-regulated (2120) in *VHL^R200W* homozygote were analyzed for enrichment in GO. On the y-axis, GO biological processes (number of differential genes covered) were ordered by adjusted *P* [60] from the most to the least significance for up-regulation or down-regulation. GO with $P_{adjusted} < 0.05$ and fold enrichment >2 are presented.

Figure 3.
Three major gene regulation modules identified from the 2932 differential genes detected between 17 *VHL* WT and 8 *VHL*^{R200W} homozygote individuals matched for serum ferritin concentration. Genes were mapped to REACTOME functional interaction database and clustered to three major regulation modules. **A-C**. Gene regulation modules 1-3, respectively. Only the hub genes, defined as the top 20% of genes with the most interacting genes within module, are presented. Yellow nodes denotes genes up-regulated in *VHL*^{R200W} homozygotes; blue nodes denote genes down-regulated; size of nodes is proportional to the number of interactions within module.

Figure 4.

Correlation between iron status as reflected in serum ferritin concentration and expression levels of VHL^{R200W} induced genes, across 24 VHL^{R200W} homozygotes (8 iron sufficient plus 16 iron deficient individuals).

A. The density distribution of Spearman's ρ between expression level and serum ferritin concentration in *VHL^{R200W}* homozygotes for genes induced (red) or suppressed (black) at FDR 0.05 and genes exhibiting no difference at this FDR (grey) by the *VHL^{R200W}* mutation. The expression of a proportion of genes up-regulated by *VHL^{R200W}* homozygosity tended to have a negative correlation with serum ferritin concentration suggesting an up regulation by iron deficiency (enhanced by low iron), while an additional proportion of genes tended to have a positive correlation with serum ferritin , suggesting a down regulation by iron deficiency (suppressed by low iron).

B. The density distribution of Spearman's ρ between gene expression level and serum ferritin concentration for genes induced in *VHL^{R200W}* homozygotes that were not (black; n =2282) or that were (red, N = 100) HIF-2 targets. HIF-2 targets that were induced in *VHL^{R200W}* homozygotes tended to have a positive correlation with serum ferritin concentration, suggesting down regulation by iron deficiency. HIF-2 targets were detected at 10% FDR in VHL−/− and HIF1A−/− renal clear cell carcinoma cell lines with and without HIF2A knocked down, using published microarray data [33].
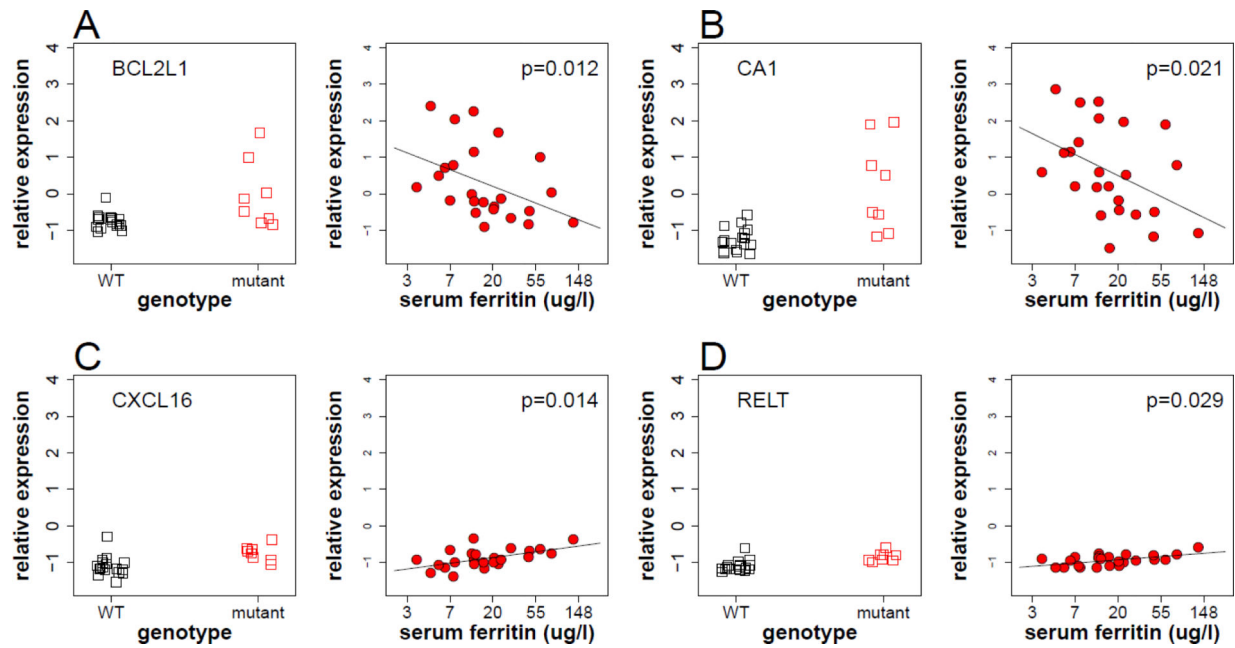
Figure 5.
Examples of homozygous VHL^{R200W}-induced genes that were modulated by iron deficiency. Four genes, *BCL2L1* (A), *CA1* (B), *CXCL16* (C) and *RELT* (D), were induced in VHL^{R200W} homozygotes (left panels), where their expression level was correlated with serum ferritin concentration (right panels). Left panel shows 17 WT individual and 8 VHL^{R200W} homozygotes matched for iron status; right panel shows 24 VHL^{R200W} homozygotes. Black points denote WT individuals and red points denote VHL^{R200W} homozygotes. *P*-values in right panels denote Spearman's rank test for correlation between gene expression level and log (ferritin) in VHL^{R200W} homozygotes.
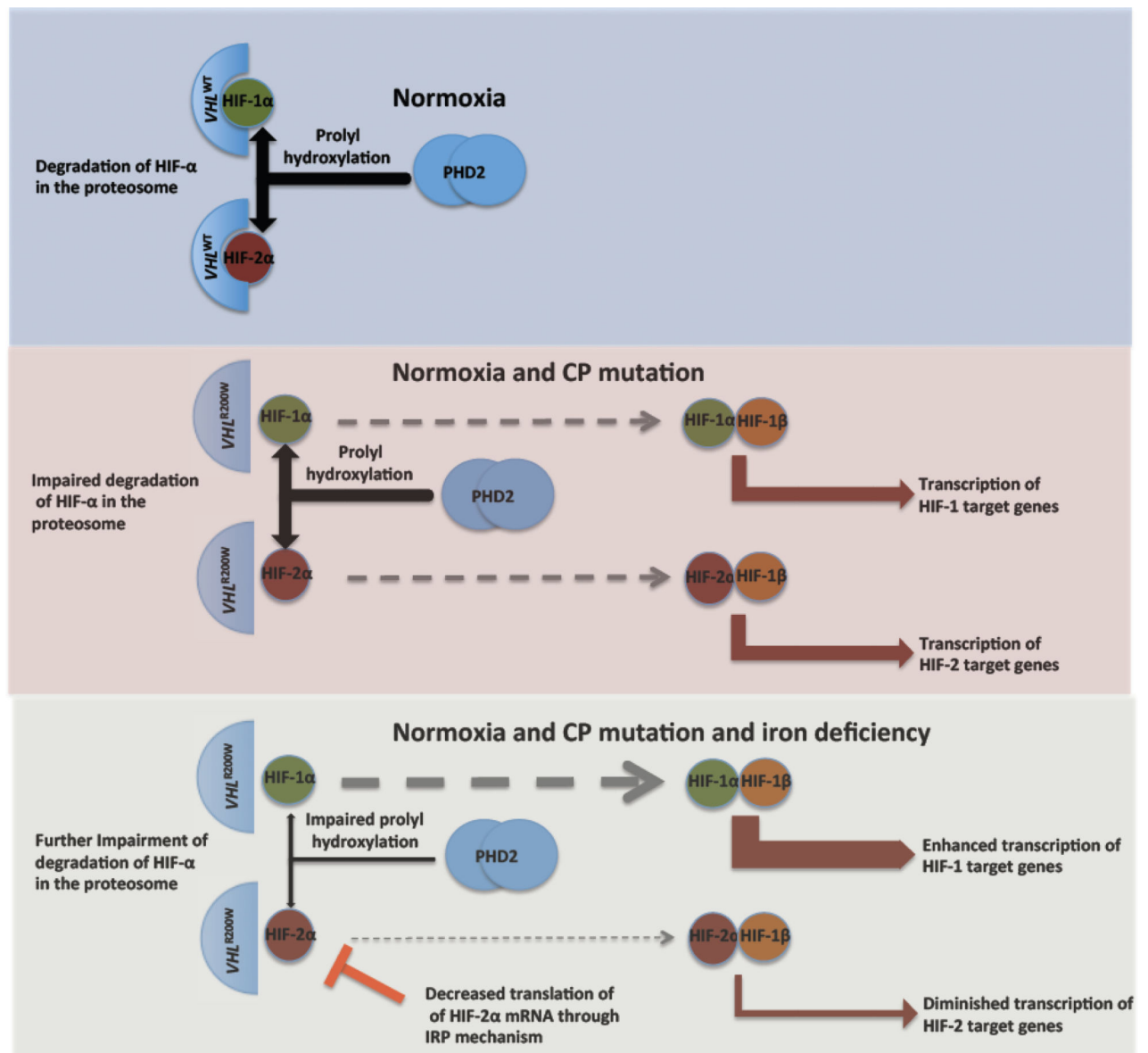
Figure 6.
Proposed mechanism for divergent expression of HIF-target genes according to iron status.
Upper panel: With non-mutated *VHL* and normal iron status in normoxia, the alpha subunits of HIF are degraded in the proteasome after prolyl hydroxylation through the action of PHD2. Middle panel: The homozygous VHL^{R200W} mutation causes impaired recognition of hydroxylated alpha-subunits of HIF, leading to increased levels of the alpha subunits of HIF and increased transcription of HIF target genes under normoxia. Lower panel: The addition of iron deficiency leads to a further increase in HIF-1α through impaired function of PHD2, but a decrease in HIF-2α because of reduced translation of HIF-2α through the interaction of iron responsive protein (IRP) with an iron response element in the 5' untranslated region of HIF-2α mRNA.

Table 1

Comparison of clinical variables in VHL^{R200W} homozygotes and VHL wildtype controls. Results in median (interquartile range) were presented unless otherwise indicated. Wilcoxon's rank sum test was applied in all comparisons except gender, which used Fisher's exact test. Subjects with ferritin concentration 21 ug/l are presented in B, where ferritin concentration ranged from 24 to 156 μg/l in control individuals and from 23 to 131 μg/l in VHL^{R200W} homozygotes (P=0.4).

	WT		VHL^{R200W}		P
	N	Median (IQR)	N	Median (IQR)	
A. All subjects					
Age (years)	21	36 (31, 54)	24	35.5 (26, 52)	0.4
Female gender n (%)	21	12 (57%)	24	15 (63%)	0.8
Systolic blood pressure (mm Hg)	21	120 (114, 125)	23	112 (105, 122)	0.1
Diastolic blood pressure (mm Hg)	21	81 (76, 85)	23	78 (72, 85.5)	0.6
Pulse pressure (mm Hg)	21	40 (35, 43)	23	39 (30, 43)	0.2
Red blood cells (1000/ul)	21	4.5 (4.2, 4.9)	24	6.9 (6.4, 7.8)	<0.001
Hemoglobin (g/dl)	21	125 (121, 139)	24	183 (155, 191)	<0.001
Hematocrit (%)	21	37.4 (36.5, 41.5)	24	56.2 (50.2, 58.6)	<0.001
Platelet (1000/ul)	21	248 (213, 301)	23	220 (189, 286)	0.3
Ferritin (ug/l)	19	58 (26, 76)	24	14 (7, 25)	0.001
Erythropoietin (IU/l)	19	7.4 (5.4, 10.5)	23	48.4 (20, 75.1)	<0.001
Vascular endothelial growth factor (pg/ml)	16	0.2 (0.2, 0.3)	23	0.2 (0.2, 5.7)	0.039
B. Subset matched for ferritin					
Age (years)	17	40 (31, 56)	8	48 (34, 53)	0.9
Female gender n (%)	17	9 (53%)	8	5 (63%)	1
Systolic blood pressure (mm Hg)	17	120 (118, 125)	8	109 (104, 126)	0.2
Diastolic blood pressure (mm Hg)	17	82 (78, 85)	8	81 (77, 91)	0.9
Pulse pressure (mm Hg)	17	40 (35, 47)	8	31 (25, 40)	0.047
Red blood cells (1000/ul)	17	4.5 (4.2, 5)	8	6.9 (6.2, 7.8)	<0.001
Hemoglobin (g/dl)	17	128 (124, 141)	8	187 (160, 191)	<0.001
Hematocrit (%)	17	39.5 (36.5, 42.8)	8	54.5 (50.2, 58.6)	<0.001
Platelet (1000/ul)	17	251 (213, 301)	8	248 (179, 292)	0.5
Ferritin (ug/l)	17	62 (29, 78)	8	46 (28, 64)	0.4
Erythropoietin (IU/l)	17	7.2 (5.4, 10.1)	8	50 (18.5, 79.3)	<0.001
Vascular endothelial growth factor (pg/ml)	12	0.2 (0.2, 0.3)	8	4.6 (0.2, 14.4)	0.025

Table 2

Genes showing at least a 1.5-fold change in regulation in VHL^{R200W} homozygotes.

Direction	Affy ID	Gene Symbol	Gene Title	Fold
up regulation	3142967	CA1	carbonic anhydrase I	2.8
	2435005	SELENBP1	selenium binding protein 1	2.3
	2571510	IL1B	interleukin 1, beta	2.2
	3759006	SLC4A1	solute carrier family 4, anion exchanger, member 1 (erythrocyte membrane protein band 3, Diego blood group)	2.1
	3360401	HBB	hemoglobin, beta	2.0
	3657253	AHSP	alpha hemoglobin stabilizing protein	2.0
	3444252	CSDA	cold shock domain protein A	2.0
	2343473	IFI44L	interferon-induced protein 44-like	1.9
	3257204	IFIT3	interferon-induced protein with tetratricopeptide repeats 3	1.8
	3203855	DCAF12	DDB1 and CUL4 associated factor 12	1.8
	3090006	SLC25A37	solute carrier family 25, member 37	1.7
	3025500	BPGM	2,3-bisphosphoglycerate mutase	1.7
	3257246	IFIT1	interferon-induced protein with tetratricopeptide repeats 1	1.7
	3360417	HBD	hemoglobin, delta	1.7
	2777714	SNCA	synuclein, alpha (non A4 component of amyloid precursor)	1.7
	3090053	SLC25A37	solute carrier family 25, member 37	1.7
	3902489	BCL2L1	BCL2-like 1	1.7
	3770345	CD300E	CD300e molecule	1.6
	2772566	IGJ	immunoglobulin J polypeptide, linker protein for immunoglobulin alpha and mu polypeptides	1.6
	3621029	EPB42	erythrocyte membrane protein band 4.2	1.6
	2353988	FAM46C	family with sequence similarity 46, member C	1.6
	3809621	FECH	ferrochelatase	1.6
	3945515	APOBEC3A	apolipoprotein B mRNA editing enzyme, catalytic polypeptide-like 3A	1.6
	3464860	DUSP6	dual specificity phosphatase 6	1.6
	3549575	IFI27	interferon, alpha-inducible protein 27	1.6
	2731513	EREG	epiregulin	1.6
	2775390	MOP-1	MOP-1	1.5
	3922100	MX1	myxovirus (influenza virus) resistance 1, interferon-inducible protein p78 (mouse)	1.5
	2896545	GMPR	guanosine monophosphate reductase	1.5
	3942531	OSBP2	oxysterol binding protein 2	1.5
	2773434	CXCL2	chemokine (C-X-C motif) ligand 2	1.5
down regulation	2496536	RPL31	ribosomal protein L31	1.8
	3031517	GIMAP7	GTPase, IMAP family member 7	1.8
	3617458	GOLGA8A /8B	golgin A8 family, member A / member B	1.7
	2781138	LEF1	lymphoid enhancer-binding factor 1	1.7

Direction	Affy ID	Gene Symbol	Gene Title	Fold
	2806468	IL7R	interleukin 7 receptor	1.6
	2821347	ERAP2	endoplasmic reticulum aminopeptidase 2	1.6
	2665199	SATB1	SATB homeobox 1	1.5
	2809793	GZMK	granzyme K (granzyme 3; tryptase II)	1.5
	2515627	ITGA6	integrin, alpha 6	1.5
	2837232	ITK	IL2-inducible T-cell kinase	1.5
	2823880	CAMK4	calcium/calmodulin-dependent protein kinase IV	1.5

Author Manuscript

Author Manuscript

Author Manuscript

Author Manuscript

Table 3

Genes for which induction by the *VHL^R200W* mutation was enhanced by low serum ferritin concentration (*P* <0.05).

Affy ID	Gene Symbol	Gene Annotation	Spearman's ρ with ferritin concentration
2353988	FAM46C	family with sequence similarity 46, member C	−0.60
3090006	SLC25A37	solute carrier family 25, member 37	−0.59
3360401	HBB	hemoglobin, beta	−0.58
3809621	FECH	ferrochelatase	−0.58
3181240	TMOD1	tropomodulin 1	−0.57
3090053	SLC25A37	solute carrier family 25, member 37	−0.57
2778856	TSPAN5	tetraspanin 5	−0.57
3263624	MXI1	MAX interactor 1	−0.57
3621029	EPB42	erythrocyte membrane protein band 4.2	−0.56
3025500	BPGM	2,3-bisphosphoglycerate mutase	−0.56
3203855	DCAF12	DDB1 and CUL4 associated factor 12	−0.56
2777714	SNCA	synuclein, alpha (non A4 component of amyloid precursor)	−0.54
2700828	SIAH2	seven in absentia homolog 2 (Drosophila)	−0.54
3759006	SLC4A1	solute carrier family 4, anion exchanger, member 1 (erythrocyte membrane protein band 3, Diego blood group)	−0.54
3855071	FKBP8	FK506 binding protein 8, 38kDa	−0.53
3759077	SLC25A39	solute carrier family 25, member 39	−0.53
3286921	MARCH8	membrane-associated ring finger (C3HC4) 8	−0.52
2435005	SELENBP1	selenium binding protein 1	−0.52
2788003	GYPA	glycophorin A (MNS blood group)	−0.52
3568534	SPTB	spectrin, beta, erythrocytic	−0.51
2451463	ADIPOR1	adiponectin receptor 1	−0.51
3902489	BCL2L1	BCL2-like 1	−0.51
2325274	C1orf128	chromosome 1 open reading frame 128	−0.51
3076178	MKRN1	makorin ring finger protein 1	−0.50
3943414	FBXO7	F-box protein 7	−0.50
3091000	BNIP3L	BCL2/adenovirus E1B 19kDa interacting protein 3-like	−0.50
3638590	MESP1	mesoderm posterior 1 homolog (mouse)	−0.49
3676165	HAGH	hydroxyacylglutathione hydrolase	−0.49
3434413	RNF10	ring finger protein 10	−0.47
3657253	AHSP	alpha hemoglobin stabilizing protein	−0.47
3142967	CA1	carbonic anhydrase I	−0.47
3550077	GLRX5	glutaredoxin 5	−0.47
3781654	RIOK3	RIO kinase 3 (yeast)	−0.47
3642654	HBM	hemoglobin, mu	−0.47

Affy ID	Gene Symbol	Gene Annotation	Spearman's ρ with ferritin concentration
3089102	EPB49	erythrocyte membrane protein band 4.9 (dematin)	−0.46
3674886	NPRL3	nitrogen permease regulator-like 3 (S. cerevisiae)	−0.46
3846783	UBXN6	UBX domain protein 6	−0.45
3360417	HBD	hemoglobin, delta	−0.45
3132940	ANK1	ankyrin 1, erythrocytic	−0.44
3444252	CSDA	cold shock domain protein A	−0.44
2438531	HDGF	hepatoma-derived growth factor	−0.43
3642687	HBQ1	hemoglobin, theta 1	−0.43
2896545	GMPR	guanosine monophosphate reductase	−0.43
3217077	HEMGN	hemogen	−0.42
3246372	NCOA4	nuclear receptor coactivator 4	−0.42
2737840	CISD2	CDGSH iron sulfur domain 2	−0.42
3373487	OR5M1	olfactory receptor, family 5, subfamily M, member 1	−0.42
3226661	ZER1	zer-1 homolog (C. elegans)	−0.42
3695867	RANBP10	RAN binding protein 10	−0.42
3890597	RBM38	RNA binding motif protein 38	−0.41

Table 4

Genes for which induction by the VHL^{R200W} mutation was repressed by low serum ferritin concentration (P <0.05).

Affy ID	Gene Symbol	Gene Annotation	Spearman's ρ with ferritin concentration
3880767	PYGB	phosphorylase, glycogen; brain	0.66
3416651	PDE1B	phosphodiesterase 1B, calmodulin-dependent	0.66
3759849	PLEKHM1	pleckstrin homology domain containing, family M (with RUN domain) member 1	0.64
3675935	CLCN7	chloride channel 7	0.63
3381241	ARAP1	ArfGAP with RhoGAP domain, ankyrin repeat and PH domain 1	0.63
3558071	RABGGTA	Rab geranylgeranyltransferase, alpha subunit	0.62
3579546	WARS	tryptophanyl-tRNA synthetase	0.61
3360006	RHOG	ras homolog gene family, member G (rho G)	0.61
3457614	CS	citrate synthase	0.61
3775038	C17orf62	chromosome 17 open reading frame 62	0.61
2489172	MTHFD2	methylenetetrahydrofolate dehydrogenase (NADP+ dependent) 2, methenyltetrahydrofolate cyclohydrolase	0.59
3337918	TPCN2	two pore segment channel 2	0.59
3449068	TMTC1	transmembrane and tetratricopeptide repeat containing 1	0.59
3188180	OR1N2	olfactory receptor, family 1, subfamily N, member 2	0.58
3760945	MRPL10	mitochondrial ribosomal protein L10	0.57
3854954	LRRC25	leucine rich repeat containing 25	0.57
3882069	MAPRE1	microtubule-associated protein, RP/EB family, member 1	0.57
3655961	PPP4C	protein phosphatase 4, catalytic subunit	0.56
3581132	AKT1	v-akt murine thymoma viral oncogene homolog 1	0.56
3009229	POR	P450 (cytochrome) oxidoreductase	0.55
3770345	CD300E	CD300e molecule	0.55
3823583	HSH2D	hematopoietic SH2 domain containing	0.55
3127199	DOK2	docking protein 2, 56kDa	0.55
3892941	OGFR	opioid growth factor receptor	0.55
3544625	FLVCR2	feline leukemia virus subgroup C cellular receptor family, member 2	0.52
2398894	RCC2	regulator of chromosome condensation 2	0.52
3849044	MYO1F	myosin IF	0.52
3529649	RNF31	ring finger protein 31	0.51
3960930	CBX6	chromobox homolog 6	0.51
3350775	SIDT2	SID1 transmembrane family, member 2	0.51
3951768	CECR1	cat eye syndrome chromosome region, candidate 1	0.51
3695699	ATP6V0D1	ATPase, H+ transporting, lysosomal 38kDa, V0 subunit d1	0.51
3933399	ZNF295	zinc finger protein 295	0.51
3841574	LILRB1	leukocyte immunoglobulin-like receptor, subfamily B (with TM and ITIM domains), member 1	0.50

Affy ID	Gene Symbol	Gene Annotation	Spearman's ρ with ferritin concentration
3090294	ADAMDEC1	ADAM-like, decysin 1	0.50
3354443	SLC37A2	solute carrier family 37 (glycerol-3-phosphate transporter), member 2	0.50
3911767	CTSZ	cathepsin Z	0.50
3389330	CASP5	caspase 5, apoptosis-related cysteine peptidase	0.50
3218528	ABCA1	ATP-binding cassette, sub-family A (ABC1), member 1	0.50
3742285	CXCL16	chemokine (C-X-C motif) ligand 16	0.49
3902682	PLAGL2	pleiomorphic adenoma gene-like 2	0.49
3577612	SERPINA1	serpin peptidase inhibitor, clade A (alpha-1 antiproteinase, antitrypsin), member 1	0.49
3337390	TCIRG1	T-cell, immune regulator 1, ATPase, H+ transporting, lysosomal V0 subunit A3	0.49
3339423	INPPL1	inositol polyphosphate phosphatase-like 1	0.49
2474977	FOSL2	FOS-like antigen 2	0.49
3833583	SHKBP1	SH3KBP1 binding protein 1	0.49
3453370	ARF3	ADP-ribosylation factor 3	0.49
3452818	VDR	vitamin D (1,25- dihydroxyvitamin D3) receptor	0.48
3833443	PLD3	phospholipase D family, member 3	0.48
3922037	MX2	myxovirus (influenza virus) resistance 2 (mouse)	0.48
3457752	STAT2	signal transducer and activator of transcription 2, 113kDa	0.48
3949162	GRAMD4	GRAM domain containing 4	0.47
3553531	TNFAIP2	tumor necrosis factor, alpha-induced protein 2	0.47
2350880	AMPD2	adenosine monophosphate deaminase 2	0.47
3598165	PLEKHO2	pleckstrin homology domain containing, family O member 2	0.47
3771602	RHBDF2	rhomboid 5 homolog 2 (Drosophila)	0.47
3293762	PSAP	prosaposin	0.47
3722338	IFI35	interferon-induced protein 35	0.47
2469213	KLF11	Kruppel-like factor 11 /// cystin 1	0.47
3529701	IRF9	interferon regulatory factor 9	0.46
3763656	TRIM25	tripartite motif-containing 25	0.46
3473727	WSB2	WD repeat and SOCS box-containing 2	0.46
3734236	TTYH2	tweety homolog 2 (Drosophila)	0.46
3934729	ITGB2	integrin, beta 2 (complement component 3 receptor 3 and 4 subunit)	0.46
3855856	LPAR2	lysophosphatidic acid receptor 2	0.45
3708874	MPDU1	mannose-P-dolichol utilization defect 1	0.45
2905327	FGD2	FYVE, RhoGEF and PH domain containing 2	0.45
3442941	C3AR1	complement component 3a receptor 1	0.45
3722917	GRN	granulin	0.45
3677516	MEFV	Mediterranean fever	0.45
3339880	RELT	RELT tumor necrosis factor receptor	0.45
3301914	PIK3AP1	phosphoinositide-3-kinase adaptor protein 1	0.45
3023246	IRF5	interferon regulatory factor 5	0.44

Affy ID	Gene Symbol	Gene Annotation	Spearman's ρ with ferritin concentration
3386737	C11orf75	chromosome 11 open reading frame 75	0.44
3824874	IFI30	interferon, gamma-inducible protein 30	0.44
3903836	EIF6	eukaryotic translation initiation factor 6	0.44
3404549	CLEC12B	C-type lectin domain family 12, member B	0.44
3720921	RARA	retinoic acid receptor, alpha	0.44
3350830	TAGLN	transgelin	0.44
3738629	SLC16A3	solute carrier family 16, member 3 (monocarboxylic acid transporter 4)	0.43
3316344	CD151	CD151 molecule (Raph blood group)	0.43
3957938	PISD	phosphatidylserine decarboxylase	0.43
3866231	STRN4	striatin, calmodulin binding protein 4	0.43
3740367	SLC43A2	solute carrier family 43, member 2	0.43
3457160	CD63	CD63 molecule	0.43
3824471	GLT25D1	glycosyltransferase 25 domain containing 1	0.42
3862650	SERTAD3	SERTA domain containing 3	0.42
3189580	ZBTB43	zinc finger and BTB domain containing 43	0.42
3881282	HM13	histocompatibility (minor) 13	0.42
3966000	TYMP	thymidine phosphorylase	0.42
3264621	TCF7L2	transcription factor 7-like 2 (T-cell specific, HMG-box)	0.42
3376529	PLA2G16	phospholipase A2, group XVI	0.42
3741769	P2RX1	purinergic receptor P2X, ligand-gated ion channel, 1	0.42
3660175	NOD2	nucleotide-binding oligomerization domain containing 2	0.42
3656829	BCKDK	branched chain ketoacid dehydrogenase kinase	0.41
3704270	CYBA	cytochrome b-245, alpha polypeptide	0.41
3708366	C17orf81	chromosome 17 open reading frame 81	0.41
3601387	PML	promyelocytic leukemia	0.41
3899173	RRBP1	ribosome binding protein 1 homolog 180kDa (dog)	0.41
3372097	ACP2	acid phosphatase 2, lysosomal	0.41
3432438	OAS1	2',5'-oligoadenylate synthetase 1, 40/46kDa	0.41
3774906	SECTM1	secreted and transmembrane 1	0.41
3709153	TMEM88	transmembrane protein 88	0.41
3855011	ELL	elongation factor RNA polymerase II	0.41
3474885	CAMKK2	calcium/calmodulin-dependent protein kinase kinase 2, beta	0.41
3861617	HNRNPL	heterogeneous nuclear ribonucleoprotein L	0.41
3813840	ZNF516	zinc finger protein 516	0.41